

Sparse Modeling of Intrinsic Correspondences

Tobias Gurdan

Computer Vision Group - Technische Universität München

Abstract

Pokrass *et al.* [PBBS⁺12] present a novel sparse modeling approach to non-rigid shape matching using only the ability to detect repeatable regions. They show that such scarce information as two sets of regions in two shapes is sufficient to establish very accurate correspondences between shapes. The paper presents methods from the field of sparse modeling and show how they can be applied to simultaneously solve for an unknown permutation ordering of the regions on two shapes and for an unknown correspondence in functional representation. It further presents numerical solutions to the resulting optimization problems. The paper also presents results and compare them to state-of-the-art methods. In this seminar paper, we give an overview on their work.

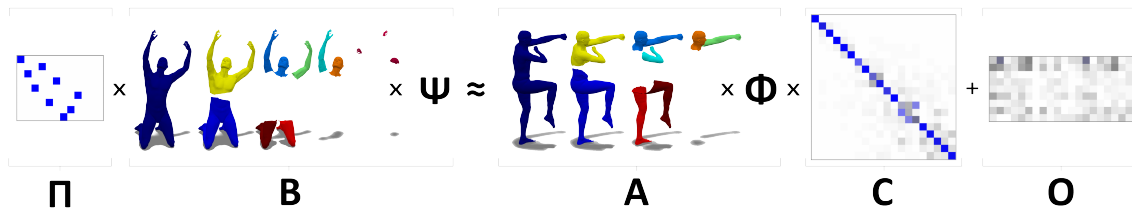


Figure 1: In their work on the *Sparse Modeling of Intrinsic Correspondences*, Pokrass *et al.* present a novel and first of its kind approach to shape matching. They show how to use tools from the field of sparse modeling to simultaneously search for an approximately diagonal \mathbf{C} and permutation $\mathbf{\Pi}$, bringing a set of regions into correspondence. The latter are given in functional representation by coefficients \mathbf{A} and \mathbf{B} . These indicator functions can represent any intrinsic property of two near-isometric shapes, e.g. repeatable regions like MSER. Such scarce information is sufficient to achieve high quality matchings with the presented robust permuted sparse coding algorithm, which outperforms state-of-the-art methods.

1 Introduction

The matching of deformable shapes is known to be a very challenging field of research. There exist numerous approaches to different subfields of shape matching, e.g. non-rigid correspondence finding or near-isometric matching [KZHCO10]. A popular approach to shape matching is to find features, that are invariant under isometric deformations and robust to noise [DMAMS10, LBB11]. There have been proposed several feature detectors, including the heat- [SOG09, GBAL09] and wave kernel signatures [ASC11] or the global point signature [Rus07]. Another approach is to embed the shapes in some higher-dimensional space, as does e.g. multidimensional scaling [EK01], spectral embedding [MHK⁺08] or the work of Lipman and Funkhouser [LF09], which use disk embeddings and Möbius transformations. More recently functional maps and the functional representation of correspondences has been introduced by Ovsjanikov *et al.* [OBCS⁺12], on which the work of Pokrass *et al.* builds upon.

The main contribution of the work of Pokrass *et al.* is an approach for finding dense intrinsic correspondences between near-isometric shapes with very little known information. It does not depend on any feature descriptors, is robust to small non-isometric deformations and very fast to compute in comparison to other methods. Additionally, it achieves better matchings compared to state-of-the-art methods in terms of relative geodesic error.

In the next section, we introduce functional maps. Followed by a short overview of sparse modeling techniques, we introduce permuted sparse coding as a tool to solve a simultaneous

permutation and correspondence problem. Afterwards, we show how to extend the simple bijective case to the more robust assumption of only having partial region correspondence. Finally, we show results and comparisons to state-of-the-art methods. We conclude with limitations and a short overview of possibilities for further improvement.

2 Functional Maps

Ovsjanikov *et al.* [OBCS⁺12] introduce functional maps as a powerful tool to compactly represent functions, e.g. point correspondences, on shapes. We will now introduce the basics of such functional representations.

Let X and Y be two shapes, modeled as compact smooth Riemannian manifolds. Let further $t : X \rightarrow Y$ be a bijective correspondence between them. Given a real function $f : X \rightarrow \mathbb{R}$, we can then construct a corresponding function $g : Y \rightarrow \mathbb{R}$ as $g = f \circ t^{-1}$. The correspondence t uniquely defines a mapping between two function spaces $T : \mathcal{F}(X, \mathbb{R}) \rightarrow \mathcal{F}(Y, \mathbb{R})$, where $\mathcal{F}(X, \mathbb{R})$ denotes the space of real functions on X . We can easily show, that T is linear, since

$$\begin{aligned} T(\alpha_1 f_1 + \alpha_2 f_2) &= (\alpha_1 f_1 + \alpha_2 f_2) \circ t^{-1} \\ &= \alpha_1 f_1 \circ t^{-1} + \alpha_2 f_2 \circ t^{-1} \\ &= \alpha_1 T(f_1) + \alpha_2 T(f_2), \end{aligned} \quad (1)$$

for every pair of functions f_1, f_2 and scalars α_1, α_2 . Assuming that X is equipped with a basis $\{\phi_i\}_{i \geq 1}$, one can represent any $f : X \rightarrow \mathbb{R}$ as $f = \sum_{i \geq 1} a_i \phi_i$, with the a_i being some representation coefficients. Mapping f to Y using the linearity of T gives

$$T(f) = T \left(\sum_{i \geq 1} a_i \phi_i \right) = \sum_{i \geq 1} a_i T(\phi_i). \quad (2)$$

If the shape Y is further equipped with a basis $\{\psi_j\}_{j \geq 1}$, one can also represent ϕ_i in terms of this basis, giving

$$T(\phi_i) = \sum_{j \geq 1} c_{ij} \psi_j, \quad (3)$$

and we can write

$$T(f) = \sum_{i,j \geq 1} a_i c_{ij} \psi_j. \quad (4)$$

We now move to a more compact notation using matrices by discretizing both the shapes and function spaces. We assume a finite sampling of X and Y , with m samples each. The bases are represented as the $m \times n$ matrices Φ and Ψ containing, respectively, n discretized functions ϕ_i and ψ_j as the columns. The functions f and $g = T(f)$ can now be represented as n -dimensional vectors $\mathbf{f} = \Phi \mathbf{a}$ and $\mathbf{g} = \Psi \mathbf{b}$. We can rewrite Equation (4) as

$$\Psi \mathbf{b} = T(\Phi \mathbf{a}) = \Psi \mathbf{C}^T \mathbf{a}. \quad (5)$$

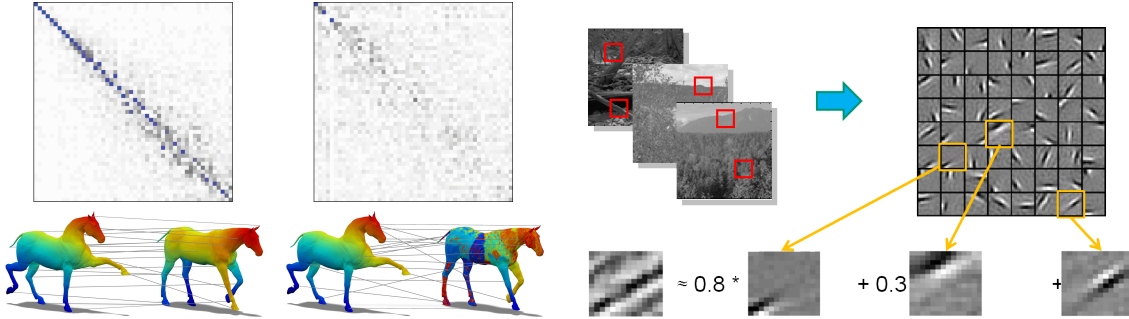
Since Ψ is invertible, we see that the following must hold.

$$\mathbf{b}^T = \mathbf{a}^T \mathbf{C}, \quad (6)$$

where \mathbf{C} is an $n \times n$ matrix that fully encodes the linear map T between the functional spaces. It contains the coordinates in the basis Ψ of the mapped elements of the basis Φ .

3 Point-to-point correspondence

Most often, one is interested in finding a point-to-point correspondence, which assumes that each point i on X corresponds to some point j on Y . In functional representation, this point-wise correspondence becomes the mapping T which relates corresponding basis vectors or respective



(a) Depicted is the matrix \mathbf{C} which encodes the bijective mapping of points between shapes. Is this mapping near-isometric, then \mathbf{C} will have near-diagonal structure. Otherwise, no constraint on the structure of \mathbf{C} can be given.

(b) In image processing, sparse coding is a powerful tool to represent image patches (upper left) using some optimized dictionary (upper right). They can be reconstructed by linearly combining the basis using the representation coefficients (bottom).

Figure 2: Left: Sparsity of \mathbf{C} for near- and non-isometric matchings. Right: Example of sparse coding in image processing.

function coefficients. In matrix notation, we look for \mathbf{C} that makes each row of $\Psi\mathbf{C}^T$ or $\mathbf{A}\mathbf{C}^T$ coincide with some row of Φ or \mathbf{B} respectively [OBCS⁺12]. If we look for a correspondence of functions represented in some basis on the two shapes, \mathbf{C} will be orthogonal and can be thought of as a rigid alignment transformation between them. Note that if we choose as bases the harmonic bases, i.e. Laplacian eigenfunctions on the two shapes, \mathbf{C} will be nearly-diagonal (cf. Figure 2a). We can solve for \mathbf{C} using the iterative closest point algorithm (ICP) in n dimensions [OBCS⁺12], initialized with the given \mathbf{C}_0 . First, find for each row i of $\Psi\mathbf{C}_0^T$ the closest row j_i^* in Φ . This can be performed efficiently using approximate nearest neighbor algorithms. Then, find an orthonormal \mathbf{C} minimizing $\sum_i \|\Phi_{j_i^*} - \Psi\mathbf{C}^T\|_2$ and set $\mathbf{C}_0 = \mathbf{C}$. This operation is repeated until convergence. As \mathbf{C} directly encodes the mapping T , one can recover the point-to-point correspondence t using e.g. indicator functions on \mathbf{C} .

4 Sparse Modeling

As mentioned in the beginning, the main contribution of the paper is the use of sparse models to optimize a specific class of functionals. We will now give a short overview on the concept of sparse modeling in general.

The central idea of sparse modeling is that many families of signals can be represented as a sparse linear combination in an appropriate domain. A common example is image compression, as e.g. done in the JPEG standard. A given image is hereby divided into 8×8 patches and each patch represented as a sparse vector of coefficients. The basis in JPEG image compression is given by the 2-dimensional discrete cosine transform, which forms 8×8 patches of the most prominent patterns occurring in natural images. These can be linearly combined to approximate any given image patch. In other words, we look for a representation of a *signal* $\mathbf{x} \approx \mathbf{Dz}$, where the basis \mathbf{D} is called *dictionary* with some representation coefficients \mathbf{z} (cf. Figure 2b). The dictionary is often selected to be overcomplete, i.e. more columns than rows (cf. [Ela10]).

There are two main problems in sparse modeling: Given a set of signals \mathbf{X} , find a dictionary \mathbf{D} that forms a solid basis. This is known as *dictionary learning*. On the other hand, given a dictionary \mathbf{D} , how to find a good representation \mathbf{z} of some signal \mathbf{x} . This is known as sparse representation *pursuit* or *sparse coding*. We now formulate the concrete problem of sparse coding.

Given some signal \mathbf{x} and a dictionary \mathbf{D} , find

$$\min_{\mathbf{z}} \|\mathbf{x} - \mathbf{Dz}\|_2^2 + \lambda \|\mathbf{z}\|_1. \quad (7)$$

This is the so-called Lasso formulation [Tib96]. The first term is the data fitting term, while the second term serves as a regularizer, imposing sparsity on \mathbf{z} . It involves the ℓ_1 norm, where

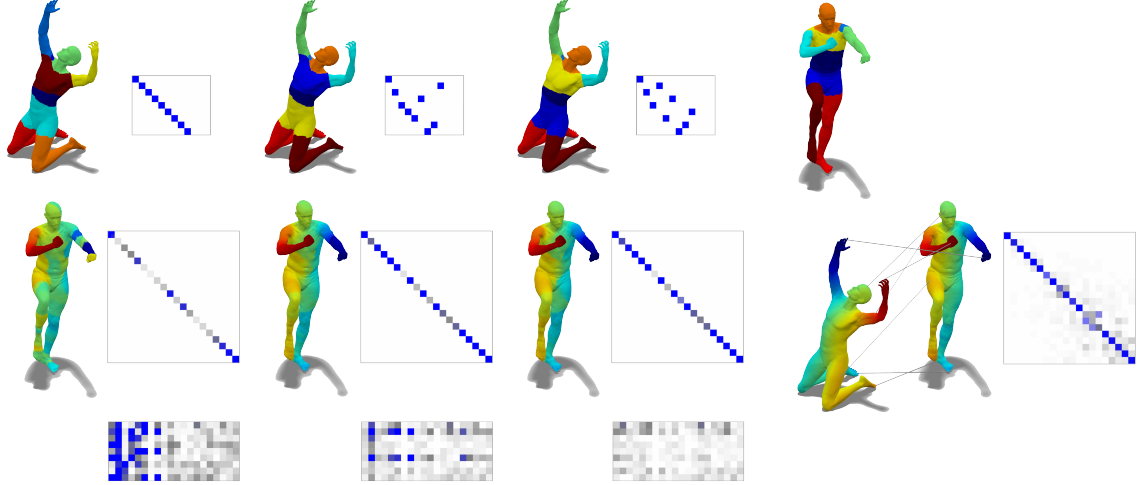


Figure 3: Three steps of the robust permuted sparse coding algorithm until convergence. Top: Permutation matrix Π and according region ordering. Middle: Correspondence in both functional (\mathbf{C}) and point-to-point representation (color-coding). Bottom: Outlier matrix \mathbf{O} .

$\|\mathbf{z}\|_1 = |z_1| + \dots + |z_n|$. Efficient algorithms to solve this optimization objective exist and are given in the next sections.

In practice it is often the case that one needs to find the representation of multiple signals \mathbf{x}_i that share some common structure. Consider a dictionary of words, containing entries in different languages. Given a set of sentences in just one of these languages, the expected representation should of course only use the basis vectors corresponding to that language, i.e. only a certain subset of columns in the dictionary is used by all signals. Stacking all conditions column-wise, we can write

$$\min_{\mathbf{Z}} \|\mathbf{X} - \mathbf{DZ}\|_F^2 + \lambda \|\mathbf{Z}\|_{2,1}, \quad (8)$$

where the first term again serves as data fitting term. The second term involves the $\ell_{2,1}$ norm, which promotes row-wise sparsity of the solution and reflects a common structure, where some columns of the dictionary are used by all signals, while others are not used at all. It is defined as $\|\mathbf{Z}\|_{2,1} = \|\mathbf{z}_1^T\|_2 + \dots + \|\mathbf{z}_m^T\|_2$, where \mathbf{z}_i^T denotes the i -th row of \mathbf{Z} .

5 Sparse Modeling of Correspondences

As mentioned in Section 3, choosing the discretized eigenfunctions of the Laplace-Beltrami operator as basis on two shapes X and Y yields a nearly diagonal, and therefore very sparse matrix \mathbf{C} . In the following, we denote the harmonic bases of X and Y by Φ and Ψ . Note that we assume simple spectra, i.e. no eigenvalues have multiplicity greater than one. Assuming isometry it follows directly, that $\Psi_i = T(\Phi_i)$ s.t. $c_{ij} = \pm \delta_{ij}$. Real-world data however is often noisy, thus we can only assume near-isometries between shapes. This leads to nearly-diagonal \mathbf{C} , whereby correspondences with low metric distortion will still give rise to sparsity its sparsity. Pokrass *et al.* take as input two near-isometric shapes and some region (or feature) detection process, that produces a collection of similar functions $f_i : X \rightarrow \mathbb{R}$ and $g_j : Y \rightarrow \mathbb{R}$. The detection process should give results based on the intrinsic properties of the shapes only to ensure similar results on near-isometric shapes. For example, the f_i 's can be indicator functions of the maximally stable regions of the shape [LBB11]. The paper first simplifies the problem by assuming perfectly repeatability in the sense that the detector finds q functions on X and Y , such that for every f_i there exists $g_j = f_i \circ t$ for an unknown correspondence t . Note, that the ordering of f_i 's and g_j 's is unknown. It can be expressed as a $q \times q$ permutation matrix Π . We represent all functions in the respective harmonic bases, thus $\mathbf{f}_i = \Phi \mathbf{a}_i$ and $\mathbf{g}_j = \Psi \mathbf{b}_j$. We stack all coefficients row-wise into $q \times n$ matrices \mathbf{A} and \mathbf{B} . Since Equation (6)

must hold for each pair of corresponding functions, we can write

$$\boldsymbol{\Pi}\mathbf{B} = \mathbf{AC}, \quad (9)$$

where $\pi_{ij} = 1$ if \mathbf{a}_i corresponds to \mathbf{b}_j and zero otherwise.

5.1 Permuted Sparse Coding

In Equation (9), both $\boldsymbol{\Pi}$ and \mathbf{C} are unknown, and solving for them is a highly ill-posed problem. However, sparse coding can be employed to exploit the sparsity of \mathbf{C} (more specifically the fact that it is nearly-diagonal). We formulate the following problem of *permuted sparse coding*

$$\min_{\mathbf{C}, \boldsymbol{\Pi}} \frac{1}{2} \|\boldsymbol{\Pi}\mathbf{B} - \mathbf{AC}\|_F^2 + \lambda \|\mathbf{W} \odot \mathbf{C}\|_1, \quad (10)$$

where the first term is the data term and the second term with the ℓ_1 regularizer promotes sparse \mathbf{C} . \odot denote element-wise multiplication and \mathbf{W} is assigned small weights w_{ij} close to the diagonal and larger weights for the off-diagonal elements, thus promoting diagonal solutions of \mathbf{C} . The minimum is sought over $n \times n$ matrices \mathbf{C} capturing the correspondence t between the shapes in functional representation and $q \times q$ matrices $\boldsymbol{\Pi}$ capturing the correspondence between the detected regions on the shapes. Equation 10 can be solved using alternating minimization iterating over \mathbf{C} with fixed $\boldsymbol{\Pi}$ and vice versa. Fixing $\boldsymbol{\Pi}$, we can denote $\mathbf{B}' = \boldsymbol{\Pi}\mathbf{B}$ and reduce problem (10) to

$$\min_{\mathbf{C}} \frac{1}{2} \|\mathbf{B}' - \mathbf{AC}\|_F^2 + \lambda \|\mathbf{W} \odot \mathbf{C}\|_1. \quad (11)$$

This is indeed similar to the Lasso problem for the pursuit of sparse representations presented in Section 4. On the other hand, fixing \mathbf{C} , we can set $\mathbf{A}' = \mathbf{AC}$ and get

$$\|\boldsymbol{\Pi}\mathbf{B} - \mathbf{A}'\|_F^2 = \text{tr}(\mathbf{B}^T \boldsymbol{\Pi}^T \boldsymbol{\Pi} \mathbf{B}) - 2\text{tr}(\mathbf{B}^T \boldsymbol{\Pi}^T \mathbf{A}') + \text{tr}(\mathbf{A}'^T \mathbf{A}'). \quad (12)$$

Since $\boldsymbol{\Pi}$ is a permutation matrix, $\boldsymbol{\Pi}^T \boldsymbol{\Pi} = \mathbf{I}$. The only non-constant term remaining in the objective is the second linear term. Problem (10) thus becomes

$$\max_{\boldsymbol{\Pi}} \text{tr}(\boldsymbol{\Pi}^T \mathbf{E}), \quad (13)$$

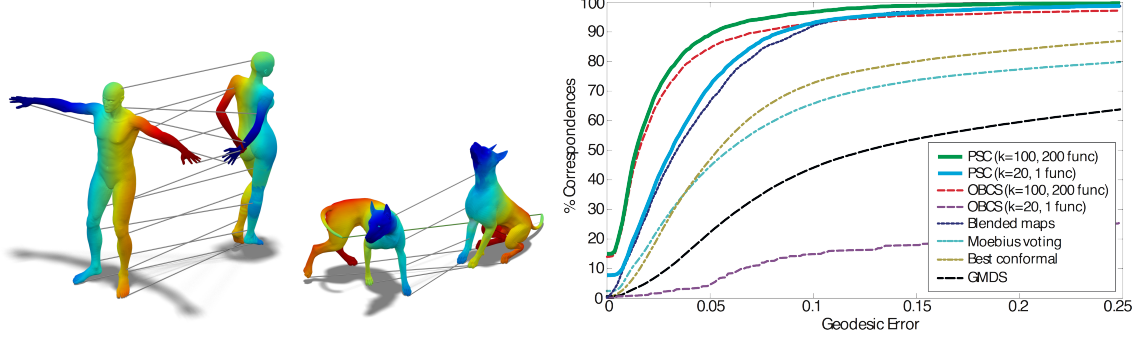
where $\mathbf{E} = \mathbf{A}' \mathbf{B}^T = \mathbf{ACB}^T$, maximizing over permutation matrices. To make it solvable using techniques from convex optimization, we relax the objective, allowing $\boldsymbol{\Pi}$ to be a double-stochastic matrix. This yields the following *linear assignment* problem:

$$\max_{\boldsymbol{\Pi} \geq \mathbf{0}} \text{vec}(\mathbf{E})^T \text{vec}(\boldsymbol{\Pi}) \quad \text{s.t.} \quad \begin{cases} \boldsymbol{\Pi}\mathbf{1} = \mathbf{1} \\ \boldsymbol{\Pi}^T \mathbf{1} = \mathbf{1} \end{cases} \quad (14)$$

Pokrass *et al.* show, that the alternating optimization of subproblems (11) and (14) converges to a local minimizer of the permuted sparse coding problem (10). Additionally, they proof, that the so recovered permutation matrix $\boldsymbol{\Pi}$ is indeed a true permutation matrix. The proof itself however is not in the scope of this summary.

5.2 Robust Permuted Sparse Coding

In the last section, we assumed a bijective correspondence between the f_i 's and g_j 's. This however is in practice not the case. The paper thus generalizes the concept of permuted sparse coding to the more realistic assumption, that q functions f_i are detected on X and r functions g_j are detected on Y , with $q \leq r$. It also assumes, that only $s \leq q$ functions f_i have a counterpart g_j . This means, that there is no correspondence between $r - s$ rows of \mathbf{B} and $q - s$ rows of \mathbf{A} . The resulting mismatched rows of \mathbf{B} can be ignored by relaxing the permutation matrix $\boldsymbol{\Pi}$ to be no more surjective. Instead of the equality constraint $\boldsymbol{\Pi}^T \mathbf{1} = \mathbf{1}$ in (14), we get $\boldsymbol{\Pi}^T \mathbf{1} \leq \mathbf{1}$. The same can be done for accounting missmatches in \mathbf{A} . However, dropping injectivity as well would result in the trivial solution $\boldsymbol{\Pi} = \mathbf{0}$.



(a) Point-to-point matching of near-isometric shapes using robust premuted sparse coding.
(b) Comparison of the presented approach to various state-of-the-art-methods.

Figure 4: Evaluation of permuted sparse coding (PSC).

For that matter, Pokrass *et al.* introduce the row-sparse $q \times n$ outlier matrix \mathbf{O} , that absorbs the $r - s$ mismatched rows of \mathbf{A} . This results in the following *robust permuted sparse coding* problem

$$\min_{\mathbf{C}, \mathbf{O}, \mathbf{\Pi}} \frac{1}{2} \|\mathbf{\Pi}\mathbf{B} - \mathbf{AC} - \mathbf{O}\|_F^2 + \lambda \|\mathbf{W} \odot \mathbf{C}\|_1 + \mu \|\mathbf{O}\|_{2,1}. \quad (15)$$

As shown in Section 4, the $\ell_{2,1}$ norm promotes row-wise sparsity, which in this case implies that the outlier matrix only contains entries where \mathbf{A} has mismatched rows. To solve objective (15), we can again alternate the optimization of two sub-problems, one with the fixed permutation $\mathbf{\Pi}$,

$$\min_{\mathbf{C}, \mathbf{O}} \frac{1}{2} \|\mathbf{B}' - \mathbf{AC} - \mathbf{O}\|_F^2 + \lambda \|\mathbf{W} \odot \mathbf{C}\|_1 + \mu \|\mathbf{O}\|_{2,1}, \quad (16)$$

where $\mathbf{B}' = \mathbf{\Pi}\mathbf{B}$, and the other one with the fixed \mathbf{C} ,

$$\max_{\mathbf{\Pi} \geq 0} \text{vec}(\mathbf{E})^T \text{vec}(\mathbf{\Pi}) \quad \text{s.t.} \quad \begin{cases} \mathbf{\Pi}\mathbf{1} = \mathbf{1} \\ \mathbf{\Pi}^T \mathbf{1} \leq \mathbf{1}, \end{cases} \quad (17)$$

where $\mathbf{E} = (\mathbf{AC})\mathbf{B}'^T$. The local convergence still holds for this generalized formulation.

5.3 Numerical Solution

The robust permuted sparse coding problem (15) can be solved using alternating optimization of a linear assignment and a sparse representation pursuit problem. The first can be tackled using the Hungarian algorithm or linear programming, the latter using a forward-backward splitting scheme. In their paper, Pokrass *et al.* sketch its derivation, which shall not be the scope of this work. We show the algorithm in its final form.

```

input : Data  $\mathbf{B}', \mathbf{A}$ ; parameters  $\lambda, \mu$ ; step size  $\alpha$ .
output : Sparse matrix  $\mathbf{O}$  and row-wise sparse outlier matrix  $\mathbf{O}$ 
Initialize  $\mathbf{O}^0 = \mathbf{B}'$  and  $\mathbf{C}^0 = \mathbf{0}$ .
for  $k=1, 2, \dots$ , until convergence do
   $\mathbf{C}^{k+1} = \mathbf{P}_1 \left( (\mathbf{I} - \frac{1}{\alpha} \mathbf{A}^T \mathbf{A}) \mathbf{C}^k - \frac{1}{\alpha} \mathbf{A}^T (\mathbf{O}^k - \mathbf{B}') \right)$ 
   $\mathbf{O}^{k+1} = \mathbf{P}_2 \left( (1 - \frac{1}{\alpha}) \mathbf{O}^k - \frac{1}{\alpha} (\mathbf{AC}^k - \mathbf{B}') \right)$ 
end

```

6 Experimental Results

In the paper of Pokrass *et al.*, they evaluate their approach on several datasets including the TOSCA [BBK08], SHREC'11 [EB] and SCAPE [ASK⁺05] datasets. Figure 4a shows exemplary results of color-coded point-to-point matchings. They calculate 5 – 15 maximally stable regions

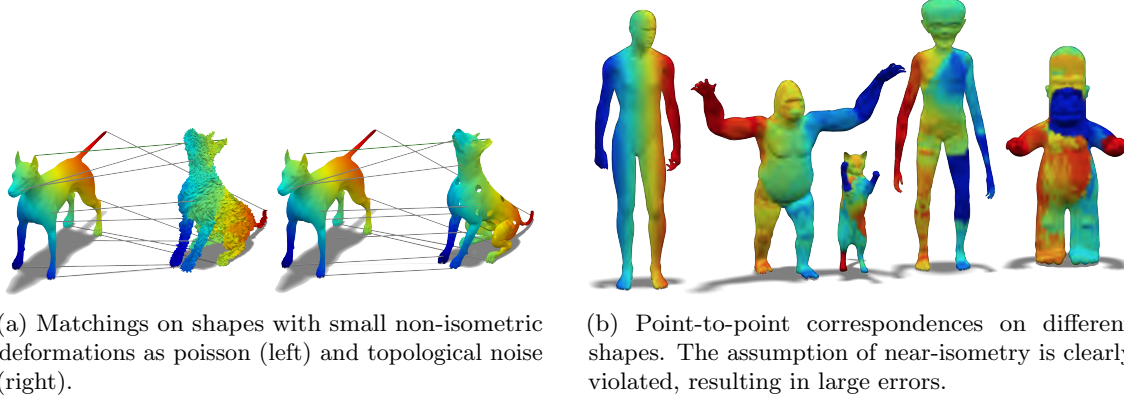


Figure 5: Limitations of permuted sparse coding.

using $6 - 10$ eigenfunctions, selecting those with at least $5 - 10\%$ of the total shape area (cf. Figure 1). The according indicator functions are projected onto 20 eigenfunctions. They initialize the permutation matrix with $\mathbf{\Pi} = \frac{1}{q}\mathbf{1}\mathbf{1}^T$ and the correspondence matrix with $\mathbf{C} = \mathbf{0}$ and solve for the corresponding matrix \mathbf{C} using the previously introduced robust permuted sparse coding algorithm. They refine the resulting \mathbf{C} using ICP as described in Section 3. The optimization of the robust permuted sparse coding objective converges after only three iterations. See Figure 3 for a visualized sequence of iterations. Table 1 shows the runtime for each of these steps on shapes of different size. Figure 4b shows a comparison to various state-of-the-art approaches, including the

Vertices	Basis	MSE _R	Opt.	Ref.	Tot.
5K	0.53	0.61	7.80	1.41	10.35
10K	0.99	1.32	7.91	2.70	12.92
20K	2.03	3.58	7.91	5.52	19.04
50K	5.57	14.23	7.85	13.99	41.64

Table 1: Runtime evaluation of permuted sparse coding.

work of Ovsjanikov *et al.* on functional maps [OBCS⁺12]. As can be seen, the presented approach clearly outperforms all state-of-the-art methods. Especially in the case of very sparse input data, i.e. about four detected regions, robust permuted sparse coding still gives very accurate matchings, while functional maps show significant distortions.

7 Limitations and Conclusion

The method introduced by Pokrass *et al.* assumes near-isometric shapes and the existance of some intrinsic similarity. While the approach works fairly well for small non-isometric deformations including gaussian and topological noise (cf. Figure 5a), it fails for clearly non-isometric shapes (cf. Figure 5b). As in such cases, the Laplacian eigenbases Φ and Ψ no longer have compatible behaviour, the sparsity of \mathbf{C} is not given any more. One possible solution, which Pokrass *et al.* plan to explore in future research, is to additionally find an appropriate basis, where \mathbf{C} has diagonal structure. This is analouge to dictionary learning from the field of sparse modeling.

To summarize, their work constitutes a novel and first of its kind approach to shape matching, that outperforms state-of-the-art methods. In their paper, they show how to use tools form sparse modeling to tackle a simultaneous search for an ordering (permutation matrix $\mathbf{\Pi}$) and assignment (correspondence matrix \mathbf{C}) of a small set of regions on two shapes in functional representation. They build upon the work of Ovsjanikov *et al.* [OBCS⁺12] and clearly outperform their results in terms of speed and quality. It also provides basis for further research and generalization, i.e. simultaneous basis optimization or shape collection matching [NBCW⁺11, KLF11].

References

- [PBBS⁺12] Jonathan Pokrass, Alexander M. Bronstein, Michael M. Bronstein, Pablo Sprechmann, and Guillermo Sapiro. Sparse modeling of intrinsic correspondences. *CoRR*, abs/1209.6560, 2012.
- [ASC11] M. Aubry, U. Schlickewei, and D. Cremers. The wave kernel signature: a quantum mechanical approach to shape analysis. In *Proc. Workshop on Dynamic Shape Capture and Analysis*, 2011.
- [ASK⁺05] D. Anguelov, P. Srinivasan, D. Koller, S. Thrun, J. Rodgers, , and J. Davis. Scape: shape completion and animation of people. In *Proceedings of the SIGGRAPH Conference*, 2005.
- [BBK06] A. M. Bronstein, M. M. Bronstein, and R. Kimmel. Generalized multidimensional scaling: a framework for isometry-invariant partial surface matching. *PNAS*, 103(5):1168–1172, 2006.
- [BBK08] A. M. Bronstein, M. M. Bronstein, and R. Kimmel. *Numerical geometry of non-rigid shapes*. Springer-Verlag New York Inc, 2008.
- [BBK⁺10] A. M. Bronstein, M. M. Bronstein, R. Kimmel, M. Mahmoudi, and G. Sapiro. A Gromov-Hausdorff framework with diffusion geometry for topologically-robust non-rigid shape matching. *IJCV*, 89(2-3):266–286, 2010.
- [DMAMS10] J. Digne, J. M. Morel, N. Audfray, and C. Mehdi-Souzani. The level set tree on meshes. In *Proc. 3DPVT*, 2010.
- [EB] M. M. Bronstein B. Bustos T. Darom R. Horaud I. Hotz Y. Keller J. Keustermans A. Kovnatsky R. Litman J. Reininghaus I. Sipiran D. Smeets P. Suetens D. Vandermeulen A. Zaharescu V. Zobel E. Boyer, A. M. Bronstein. Shrec 2011: robust feature detection and description benchmark. In *EUROGRAPHICS Workshop on 3D Object Retrieval (3DOR)*.
- [EK01] A. Elad and R. Kimmel. Bending invariant representations for surfaces. In *Proc. CVPR*, pages 168–174, 2001.
- [Ela10] M. Elad. *Sparse and Redundant Representations: From Theory to Applications in Signal and Image Processing*. Springer, 2010.
- [GBAL09] K. Gebal, J. Andreas Bærentzen, H. Aanæs, and R. Larsen. Shape analysis using the auto diffusion function. *Comput. Graph. Forum*, 28(5):1405–1413, 2009.
- [KLF11] V. G. Kim, Y. Lipman, and T. Funkhouser. Blended intrinsic maps. *TOG*, 30(4):79, 2011.
- [KZHC010] O.V. Kaick, H. Zhang, G. Hamarneh, and D. Cohen-Or. A survey on shape correspondence. In *Computer Graphics Forum*, volume 20, pages 1–23, 2010.
- [LBB11] R. Litman, A. M. Bronstein, and M. M. Bronstein. Diffusion-geometric maximally stable component detection in deformable shapes. *Computers & Graphics*, 35(3):549 – 560, 2011.
- [Lév06] B. Lévy. Laplace-beltrami eigenfunctions towards an algorithm that understands geometry. In *Proc. SMI*, 2006.
- [LF09] Y. Lipman and T. Funkhouser. Möbius voting for surface correspondence. *ACM Transactions on Graphics (Proc. SIGGRAPH)*, 28(3), August 2009.
- [MHK⁺08] Diana Mateus, Radu P. Horaud, David Knossow, Fabio Cuzzolin, and Edmond Boyer. Articulated shape matching using laplacian eigenfunctions and unsupervised point registration. In *Proc. CVPR*, 2008.

- [NBCW⁺11] A. Nguyen, M. Ben-Chen, K. Welnicka, Y. Ye, and L. Guibas. An optimization approach to improving collections of shape maps. In *Computer Graphics Forum*, volume 30, pages 1481–1491, 2011.
- [OBCS⁺12] M. Ovsjanikov, M. Ben-Chen, J. Solomon, A. Butscher, and L. Guibas. Functional maps: A flexible representation of maps between shapes. *TOG*, 31(4), 2012.
- [Rus07] R. M. Rustamov. Laplace-beltrami eigenfunctions for deformation invariant shape representation. In *Proc. of SGP*, pages 225–233, 2007.
- [SOG09] J. Sun, M. Ovsjanikov, and L. J. Guibas. A concise and provably informative multi-scale signature based on heat diffusion. In *Proc. SGP*, 2009.
- [Tib96] R. Tibshirani. Regression shrinkage and selection via the LASSO. *J. Royal Stat. Society: Series B*, 58(1):267–288, 1996.